MIDDLE EAST TECHNICAL UNIVERSITY

Pre-Outburst *Chandra* Observations of the Recurrent Nova T Pyx

ŞÖLEN BALMAN

Department of Physics, Middle East Technical University, Inonu Bulvari, Ankara, Turkey

SUMMARY

I present a total of 98.8 ksec ($\sim$ 3×30 ksec) observation of the recurrent nova T Pyx obtained with the ACIS-S3 detector on-board the Chandra Observatory during the quiescent phase of the nova before its outburst in April 2011. The total spectrum from the source T Pyx gives a maximum temperature kT$_{max}>$ 37.0 keV (2σ lower limit) with (0.9-1.5)$\times10^{-13}$ erg s^{-1} cm^{-2} and (1.3-2.2)$\times10^{32}$ erg s^{-1} (at 3.5 kpc) in the 0.1-50 keV range using a multiple-temperature plasma emission model with a power law distribution of temperatures (i.e., CEVMKL in XSPEC). I find a ratio of (L$_x$/L$_{disk}$)$\simeq$(2-7)$\times10^{-4}$ and the ratio is smaller if L$_{disk}$ is higher than 3$\times10^{35}$ erg s^{-1} indicating considerable inefficiency of emission in the boundary layer. There is no soft X-ray blackbody emission from T Pyx with a 2σ upper limit on the blackbody temperature and the flux/luminosity as kT$_{BB}<$ 25 eV and L$_{soft}<$ 2.0$\times10^{33}$ erg s^{-1} in the 0.1-10.0 keV band. All fits yield only interstellar N$_{\rm H}$ during quiescence. I suggest that T Pyx has an optically thin boundary layer merged with an ADAF-like flow (Advection-Dominated Flow) and/or X-ray corona in the inner disk indicating ongoing quasi-spherical accretion at (very) high rates during quiescent phases. The central source (i.e., the binary system) emission and its spectrum has been deconvolved from any possible extended emission with a long and detailed procedure at the sub-pixel level revealing an extended emission at S/N of $\sim$7-10. The derived shape looks like an elliptical/ring with an outer radius $\sim$0.9 arcsec and an inner radius of $\sim$0.45 arcsec, also indicating an elongation towards south. The count rate in the extended emission is $<$0.0025 c s^{-1} . The luminosity of the nebula is $\sim$(0.6-30.0)$\times10^{31}$ erg s^{-1} (at 3.5 kpc). The nebulosity seems consistent with an interaction of the outflow/ejecta from the 1966 outburst.

1 Introduction

Classical novae are a subset of cataclysmic variables which are interacting binary systems hosting a main-sequence secondary (sometimes a slightly evolved star) and a primary component, a white dwarf (Warner 1995). An outburst on the surface of the white dwarf as a result of a thermonuclear runaway in the accreted material causes the ejection of 10^{-3} to 10^{-7} M$_\odot$ of material at velocities up to several thousand kilometers per second (Shara 1989; Livio 1994; Starrfield 2001).

In non-magnetic CVs (T Pyx is known to belong to this class), the accreting material creates a boundary layer (BL) which is the transition region between the disk and the WD. Standard accretion disks half of the accretion luminosity is dissipated from the disk in the optical and UV wavelengths and the other half emerges from the boundary layer as X-ray and extreme UV (EUV)/soft X-ray emission (Lynden-Bell & Pringle 1974).

T Pyx had five outbursts in 1890, 1902, 1920, 1944, and 1966 with an inter outburst time of 19$\pm$5.3 yrs (Webbink et al. 1987). A recent quite delayed outburst occurred on April 14, 2011 (Waagan et al. 2011) and was observed over the entire electro-magnetic spectrum including the X-rays (e.g, Tofflemire et al. 2013, Chomiuk et al. 2014, Nelson et al. 2014). Ground-based optical imaging of the shell of T Pyx shows expansion velocities of about 350-500 km s^{-1} (Shara et al. 1989; O'Brien & Cohen 1998). *Hubble Space Telescope* (HST; 1994-2007) observations of the shell show thousands

of knots in Hα and [NII] with expansion velocities of 500-715 km s^{-1} that have not decelerated and the main emission is within a radius of 5″-6″ (Shara et al. 1997; Schaefer, Pagnotta & Shara 2010). The spectral energy distribution (SED) is dominated by an accretion disk in the UV+opt+IR ranges, with a distribution (after correction for reddening) that is described by a power law F_λ=4.28$\times$10^{-6} $\lambda^{-2.33}$ erg s^{-1} cm^{-2} $\mathring{A}^{-1}$, while the continuum in the UV range can also be represented by a single blackbody of T$\sim$ 34,000 K with $\dot{M}$ $\sim$ (1-4)$\times$10^{-8} M$_\odot$ yr^{-1} (Gilmozzi & Selvelli 2007; Selvelli et al. 2008).

2 Data and Observations

T Pyx was observed using the Chandra (Weisskopf, O'dell, & van Speybroeck 1996) Advanced CCD Imaging Spectrometer (ACIS; Garmire et al. 2000) for a total of $\sim$ 98.8 ksec on three different pointings: 2011 January 31 (UT 16:22:36), 2011 February 2 (UT 03:05:41), and 2011 February 5 (UT 22:33:52) (PI=S. Balman). I used S3 (the back-illuminated CCD) with the FAINT mode, and no gratings, yielding a moderate non-dispersive energy resolution. The pipeline-processed data (aspect-corrected, bias-subtracted, graded and gain-calibrated event lists) are used for the analysis, and *acis-process-events* thread is used to double check/reprocess the level 1 data using the necessary calibration files with the aid of CIAO 4.3 and CIAO 4.4 using CALDB 4.4.2-4.4.8 . Some of the preliminary results regarding any extended emission can be found in Balman et al. (2012).

3 Spectral Analysis and Results

To obtain a total spectrum from the three data sets of T Pyx CIAO task *specextract* and *combine-spectra* is used. The X-ray spectra of CVs are rich in emission lines of H- and He-like elements and Fe L-shell lines, indicating a hot, optically thin plasma with large range of temperatures (see also Balman 2012). The X-ray spectra of nonmagnetic CVs are modeled with multi-temperature isobaric cooling flow type models (as in MKCFLOW or CEVMKL within XSPEC software) and found consistent (Mukai et al. 2003, Baskill et al. 2005, Pandel et al. 2005, Guver et al. 2006, Okada et al. 2008, Balman et al. 2011). The combined spectrum of T Pyx can not be fitted with a single-temperature component plasma emission model in collisional equilibrium or a blackbody model, with χ^2_ν values much larger than 2. CEVMKL in $XSPEC$, has been used to model the spectrum of T Pyx in accordance with the general concensus of the X-ray spectra of nonmagnetic CVs (see Table 1 and Figure 1).

Table 1: Spectral Parameters of the Total Combined Chandra **data**

	CEVMKL[§1]	MEKAL[§2]
N_{H1} ($\times10^{22}$ cm^{-2})	$0.08^{+0.10}_{-0.05}$	$0.3^{+0.2}_{-0.2}$
α	$0.7^{+0.3}_{-0.2}$	N/A
kT_1 (keV)	N/A	$0.25^{+0.13}_{-0.05}$
kT_{max} (keV)	47.0<	N/A
K_{cevmkl} ($\times10^{-5}$ cm^{-5})	$4.4^{+0.7}_{-0.4}$	N/A
K_{mekal}[§3] ($\times10^{-6}$ cm^{-5})	N/A	$4.0^{+2.4}_{-2.0}$
kT_2 (keV)	N/A	22<
K_{mekal}[§3] ($\times10^{-5}$ cm^{-5})	N/A	$3.7^{+0.4}_{-1.7}$

Notes. §1 The model is (*tbabsCEVMKL); *tbabs*–Wilms et al. 2000; CEVMKL is a multi-temperature plasma emission model built from the mekal code. Emission measures follow a power-law in temperature (dEM = (T/Tmax)$^{\alpha-1}$ dT/Tmax). §2 The model is (*tbabs**(MEKAL+MEKAL)); MEKAL–Mewe et al. 1986. §3 The normalization constant of the MEKAL plasma emission models is**

K=($10^{-14}/4\pi D^2$)$\times$EM where EM (Emission Measure) =$\int n_e\ n_H\ dV$ (integration is over the emitting volume V). !

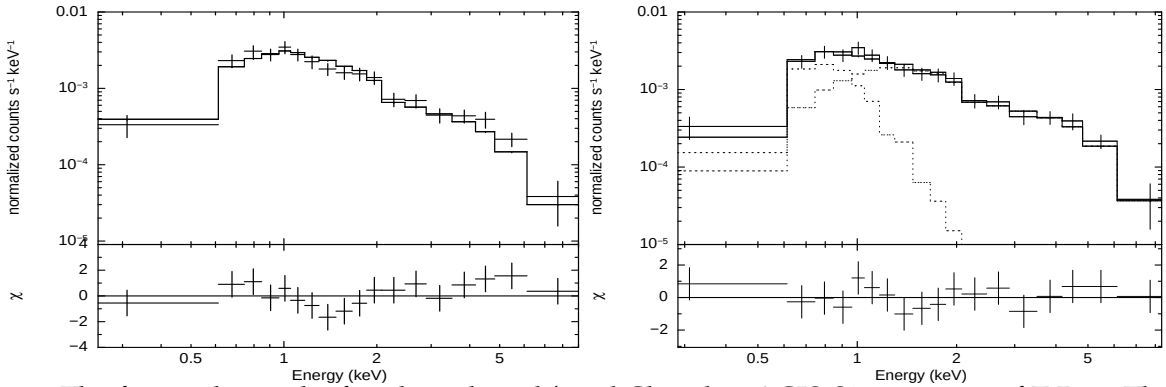

Figure 1: The figure shows the fitted combined/total Chandra ACIS-S3 spectrum of T Pyx. The top panel is the fit with the $tbabs\times$CEVMKL model and the bottom panel shows the fitted $tbabs\times$(MEKAL+MEKAL) model. The crosses are the data with errors, solid lines are the fitted model and dotted lines show the contribution of the models. The lower panels show the residuals in standard deviations (in sigma).

4 Temporal Analysis of the Source

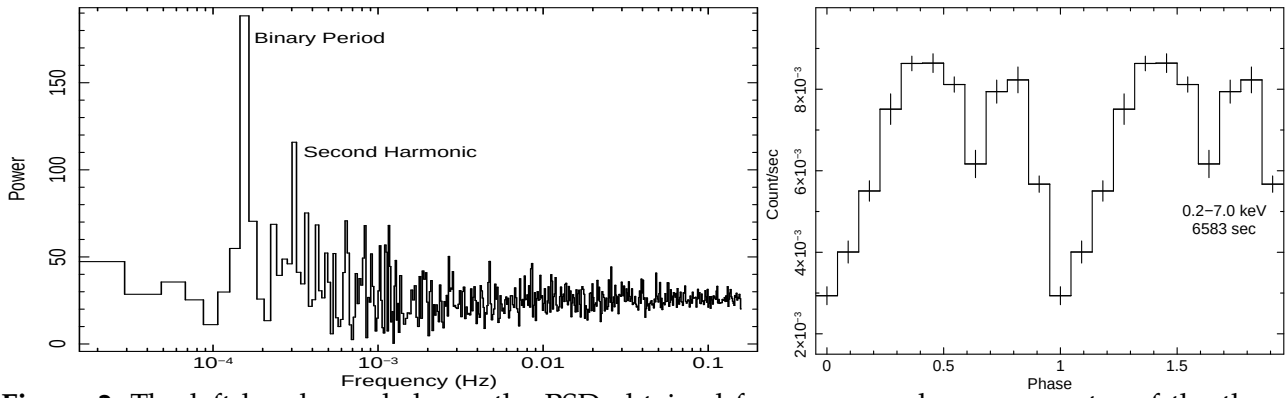

Figure 2: The left hand panel shows the PSD obtained from averaged power spectra of the three observations. The right hand panel is the folded average X-ray light curve of T Pyx using the detected binary period.

I created background-subtracted light curves with the aid of the CIAO task *dmextract* to search for any time variability. I find significant modulations at the binary period of the system (and its second harmonic) above 99.9% confidence level where 3σ power threshold is > 77 taking into account the red noise in the PDS around the binary period and its harmonic. The binary period is 1.8295(3) hrs; 0.152 mHz (Uthas et al. 2010). I do not detect any other periodicity. The PDS with the detected period of 0.155$\pm$0.005 mHz is displayed in Figure 2. Energy dependence of these orbital modulations are studied using light curves in the 0.2-1.0 and 1.0-2.0 and 2.0-7.0 keV energy bands. Aside from the changing average count rates in the energy ranges, the modulations and the shape of the average light curve are unaltered. There is no energy dependence in the orbital modulations in the Chandra energy band.

5 On the Extended Emission

A low S/N ($\sim$ 4-5σ) extended excess emission was recovered in the XMM-$Newton$ data of T Pyx (Balman 2010). To improve the spectral statistical quality and effectively recover the extended emission using deeper imaging, the three Chandra observations of T Pyx were merged with the standard procedures (see http://cxc.harvard.edu/ciao/threads/combine/). In merging events, there are two important factors, one is the fine astrometric shifts that are necessary to match sources, the second is the choice of a common tangent plane as used in this analysis with the assumed new RA-DEC position to project all the events files. To create the PSF the CHART ray tracer was utilized using the necessary off axis angles (taken from the merged event file), the combined source spectrum and the entire exposure time (98.8 ksec). Next, MARX version 4.5.0 was used to project the PSF rays onto the detector plane and finally an events file was generated for the source PSF. Since the standard Chandra pixel resolution did not properly resolve the structure of the extended emission, a 0.1 pixel resolution (sub-pixel resolution) was assumed for a detailed imaging analysis.

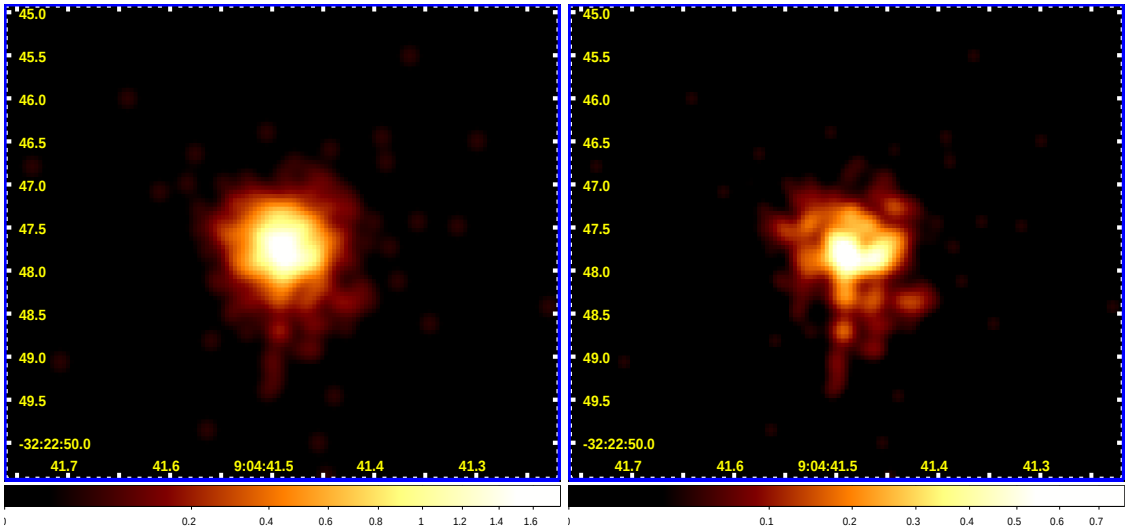

Figure 3: X-ray images of T Pyx Nebula in the 0.2 to 7.0 keV range. The resolution is 0.″15 per pixel. North is up and West is to the right. The top panel is the image without the subtraction of the central source PSF. The bottom panel is the PSF-subtracted image. The axes on the figures show RA (x-axis) and DEC (y-axis). The images utilize different brightness levels using the squate root scaling.

A PSF sub-image with the same spatial resolution is subtracted from the same sub-image of the merged events file with matched coordinates (see Figure 3). The PSF-subtracted final image indicates some extended emission with an elliptical shape. The inner semi-major axis is $\sim$ 0″.45 and the outer semi-major axis is $\sim$ 0″.9 . The inner semi-minor axis is $\sim$ 0″.2 and the outer semi-minor axis is $\sim$ 0″.4. This indicates a torus-like or ring-like structure around the nova. There is also an elongation towards the south to about 1″.85 from the point source. The southern extension comprises about 13% of the extracted X-ray nebulosity. The count rate of the nebulosity is $\sim$ (0.0025-0.0015) c s^{-1} . The signal-to-noise ratio is between 7-10 using S/N=E/$\sqrt{(B+P)}$; E is the net nebular counts, B is the background counts and P is the counts in the PSF. Detailed radial surface brightness profiles of the source indicates the extended emission as well as (see Figure 4).

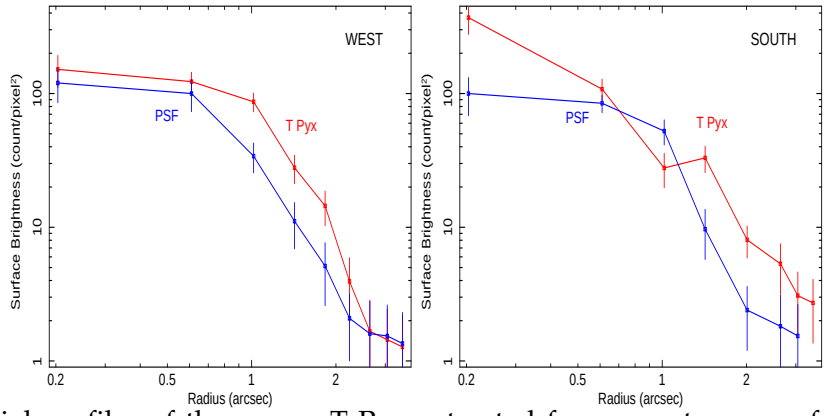

Figure 4: The radial profiles of the source T Pyx extracted from a sector-area of opening angle 30 degrees. From the left hand to the right hand panel the profiles are in the western, and southern directions, respectively. In all panels, an equivalent Chandra ACIS-S3 PSF radial profile of about 500 photons calculated from the same sector is overplotted. Gaussian errors are assumed.

Table 2: Spectral Parameters of the Nebular Spectrum of T Pyx (0.2-9.0 keV); ranges correspond to 2σ errors (Δ= 3.84 – single parameter) for the first and 3σ errors (Δ= 6.63 – single parameter) for the second component; χ^2_ν values of the fits are $\leq$ 1.0.

	PSHOCK[§1]	MEKAL[§2]
N_{H1} ($\times 10^{22}$ cm^{-2})	$0.4^{+0.25}_{-0.2}$	$0.5^{+0.4}_{-0.3}$
kT_{s1} (keV)	$1.0^{+1.1}_{-0.4}$	$0.6^{+0.3}_{-0.3}$
τ_1 (τ=n$_0$t) ($\times 10^{11}$ s cm^{-3})	$\sim$3.2	N/A
K_1[§3] ($\times 10^{-5}$ cm^{-5})	$0.6^{+0.3}_{-0.5}$	$0.6^{+0.3}_{-0.3}$
N_{H2} ($\times 10^{22}$ cm^{-2})	$11.5^{+22.5}_{-7.3}$	$17.0^{+9.7}_{-14.0}$
kT_{s2} (keV)	2.3<	$2.2^{+2.0}_{-1.2}$
τ_2 (τ=n$_0$t) ($\times 10^{11}$ s cm^{-3})	$\sim$2	N/A
K_2[§3] ($\times 10^{-5}$ cm^{-5})	$3.5^{+5.2}_{-1.7}$	$9.8^{+23.0}_{-7.5}$

Notes. §**1** The model is (*tbabs**PSHOCK+*tbabs**PSHOCK); *tbabs*–Wilms et al. 2000; PSHOCK–Borkowski et al. 2001. §**2** The model is (*tbabs**MEKAL+*tbabs**MEKAL); MEKAL–Mewe et al. 1986. §**3** Fit normalizations; a propagated count rate error of 40% is quadratically added. The normalization constant of the MEKAL/PSHOCK plasma emission models is K=($10^{-14}/4\pi D^2$)$\times$EM where EM (Emission Measure) =$\int n_e\, n_H\, dV$ (integration is over the emitting volume V).

The nebular emission is less than 2″ around the point source and a successful deconvolution of the spectrum of the nebular emission and the point source can not be done using the standard techniques using CIAO. Several images were created at given Chandra channel ranges for the source and the PSF and finally images were subtracted and resulting photons were used to calculate deconvolved nebular spectrum. The spectra and fitted spectrum are given in Figure 5. The spectral parameters of the nebula are in Table 2.

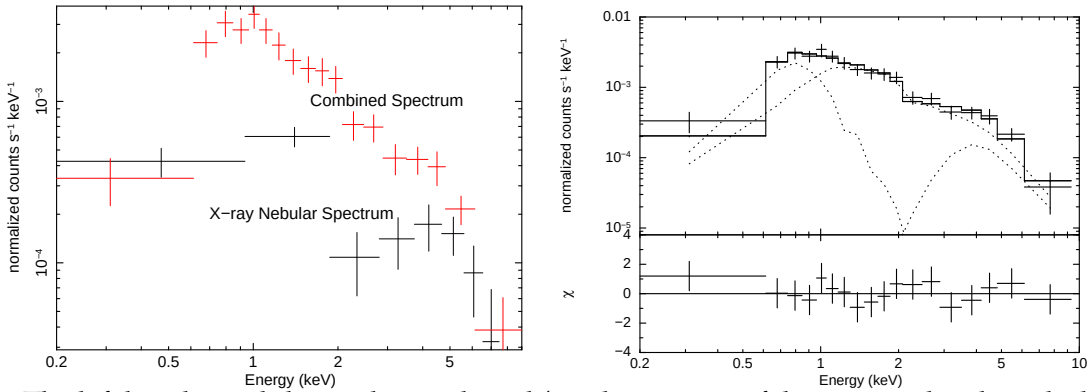

Figure 5: The left hand panel shows the combined/total spectrum of the source plus the nebular emission in the X-rays (in red) and the nebular X-ray spectrum of T Pyx (in black). The right hand panel shows the Chandra ACIS-S3 combined spectrum fitted with (*tbabs**(MEKAL+MEKAL)+*tbabs**MEKAL) model of emission. The dotted lines show the contribution of the three fitted MEKAL models two of which fits the X-ray nebular spectrum and the third fits the central source spectrum. The lower panel shows the residuals in standard deviations (in sigma).

6 Discussion and Conclusions

- The total source spectrum is consistent with a multi-temperature (distribution) thermal plasma emission model (e.g. CEVMKL) (rather than a single temperature thermal plasma (e.g. MEKAL) or a single power law model) with a maximum temperature kT$_{max}$ > 47.0 keV (2σ lower limit is 37 keV). The maximum plasma temperatures are virialized and thus, the plasma is likely not confined to the disk. The absorption towards the source is at the interstellar level consistent with the E(B-V) values as determined from the X-ray fits.

- The standard disk theory at steady state with constant $\dot{M}$ predicts, an optically thick boundary layer at the accretion rate of T Pyx as determined from the optical and UV bands ($\dot{M} \geq \times 10^{-8}$ M$_\odot$ yr^{-1}), with a blackbody emission in the soft X-ray/EUV regime. I find no such emission with a 2σ upper limit to the blackbody temperature kT$_{BB}$<25 eV and unabsorbed flux <1.5$\times$ 10^{-12} erg s^{-1} cm^{-2} at L$_{BB}$<2.0$\times10^{33}$ erg s^{-1} (0.1-10.0 keV). This result is consistent with all such results attained from X-ray wavelengths.

- The X-ray to disk luminosity ratio of T Pyx is (L$_x$/L$_{disk}$)$\simeq$(2-7)$\times10^{-4}$ given an L$_{disk}$ of 3$\times10^{35}$ erg s^{-1} and the ratio will be even lower for any L$_{disk}$ larger than this. These results strongly indicate that the boundary layer of T Pyx is non-standard.

- A detailed subpixel imaging analysis indicates excess emission around T Pyx with S/N (7-10) as an elliptical ring-like (or torus-like) nebulosity with a semi-major axis $\sim$ 0.9 arc sec and semi-minor axis $\sim$ 0.45 arc sec. There is some elongation towards south ($\sim$ 1.85 arc sec), as well. The north-south inclination angle of the elliptical ring is $i \leq 27^\circ$. The extended emission excess shows emission from plasma in ionization equibrium or close to equilibrium. An observation of T Pyx which is significantly longer and uninterrupted, and pointed at the nominal point of Chandra ACIS-S can resolve the possible positional uncertainities in allignment and justify the subpixel analysis method that can confirm the evident characteristics of the nebulosity.